

Supplement

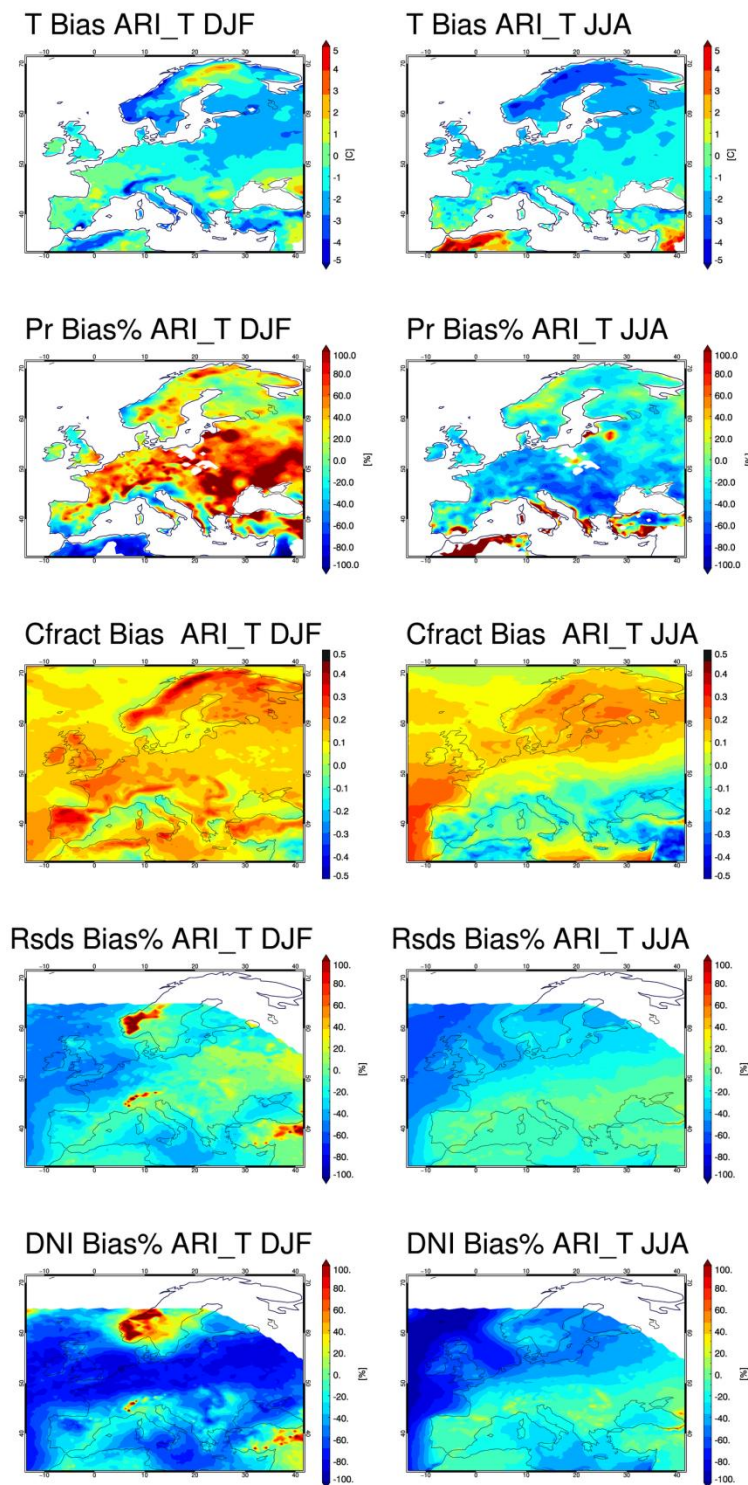


Figure S1: Bias plots for control simulation ARI_T for winter (DJF-left) and summer (JJA-right). Biases depicted from top to bottom for temperature (T), precipitation (Pr), total cloud fraction (Cfrac), down welling shortwave radiation to the surface (Rsds) and direct normalized irradiance at the surface (DNI).

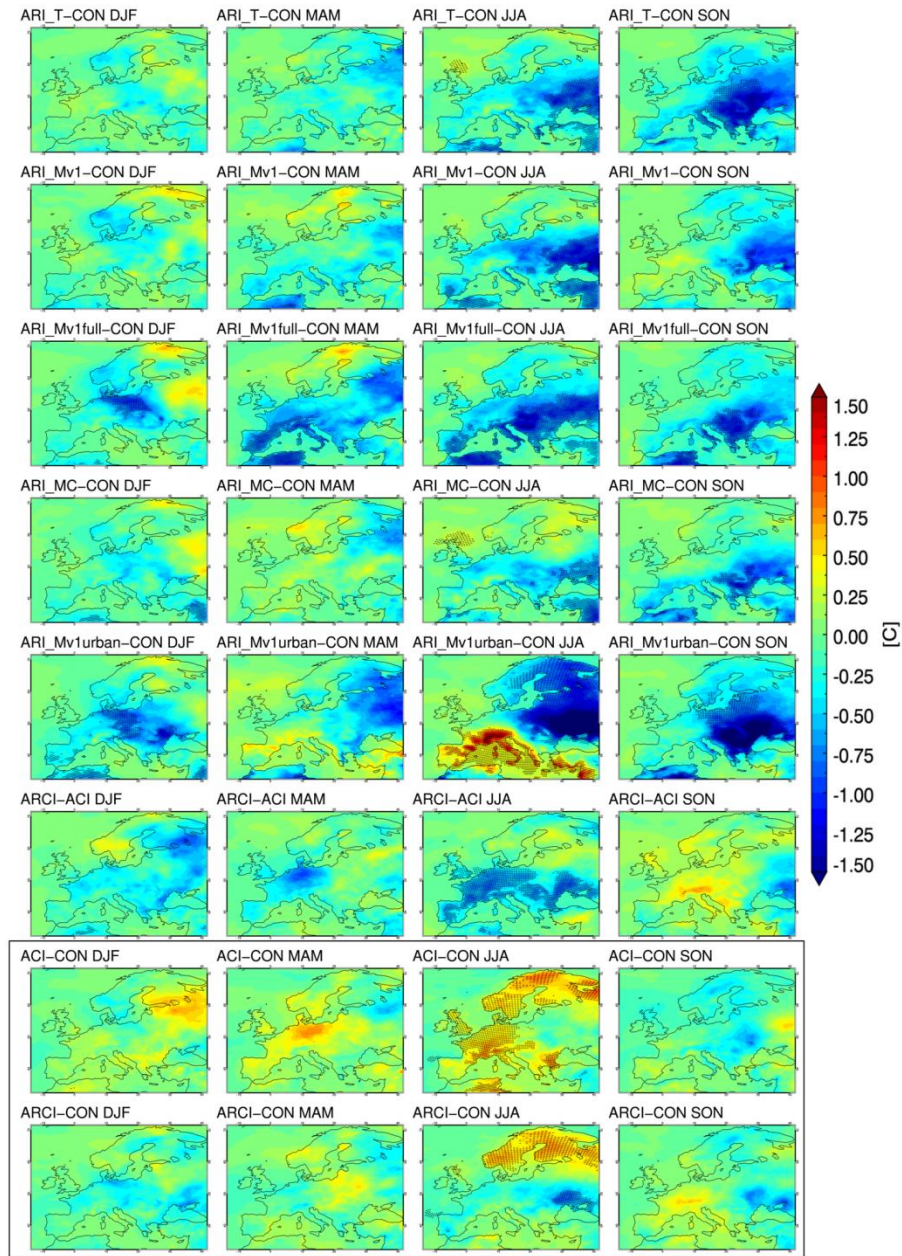


Figure S2: Near-surface temperature (T) changes from control simulation CON for all experiments and seasons. Furthermore the temperature difference of ARCI calculated against ACI (ARCI-ACI) is given to assess aerosol-radiation interactions implementation in the Thompson aerosol-interacting cloud microphysics (TE2014) (row six). First six rows present the impact of aerosol-radiation interactions. Last two rows (black box) present the impact of TAER with indirect effect against control (row seven) and TE with aerosol-radiation interactions enabled against control (row eight). Stippling indicates areas where the differences are statistically significant at the 95% level, according to the Mann-Whitney non parametric test.

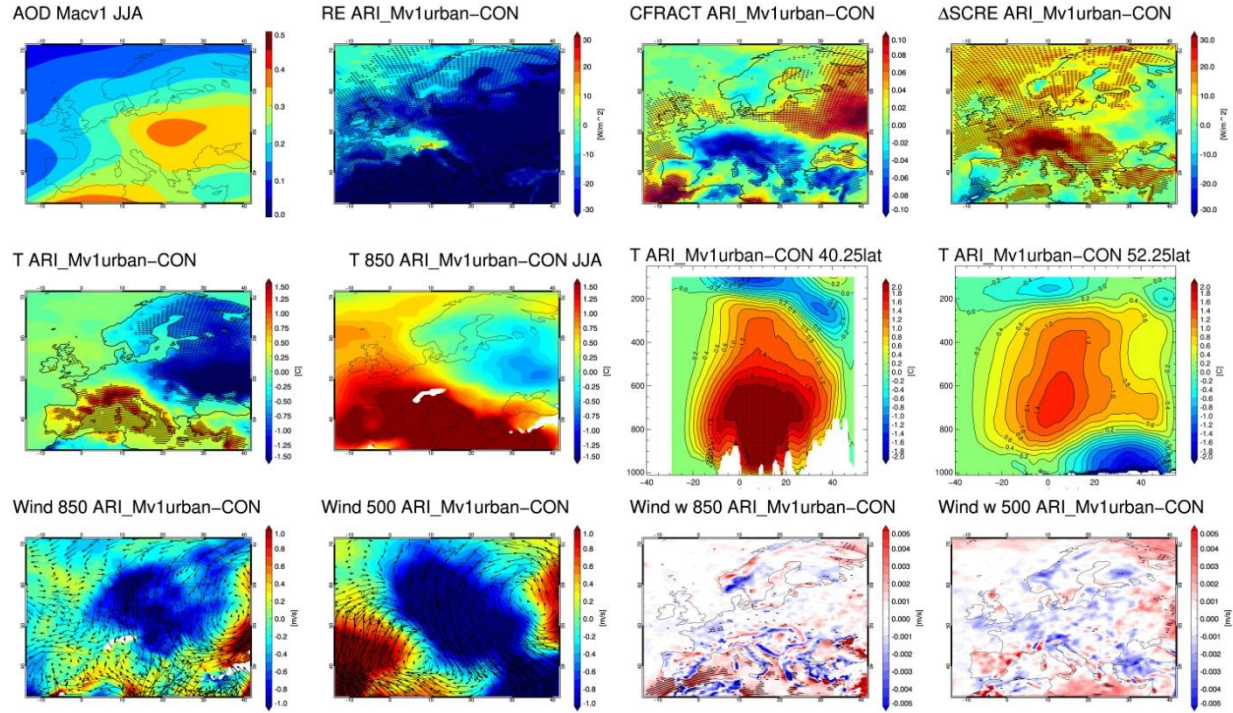


Figure S3: Composite analysis for ARI_Mv1urban in JJA. All differences are calculated from CON. Top row, from left to right: AOD field, Radiative forcing RE, difference in cloud fraction CFRACT, difference in cloud forcing SCRE. Second row: Difference in near-surface temperature (TAS), Temperature differences at 850hPa, cross-section at 40.25 latitude depicting differences in temperature vertical profile, cross-section at 50.25 latitude depicting differences in temperature vertical profile. Bottom row: difference at the wind field at 850hPa and 500hPa, difference in vertical wind speed w at 850hPa and at 500hPa. Stippling indicates areas of statistical significance.

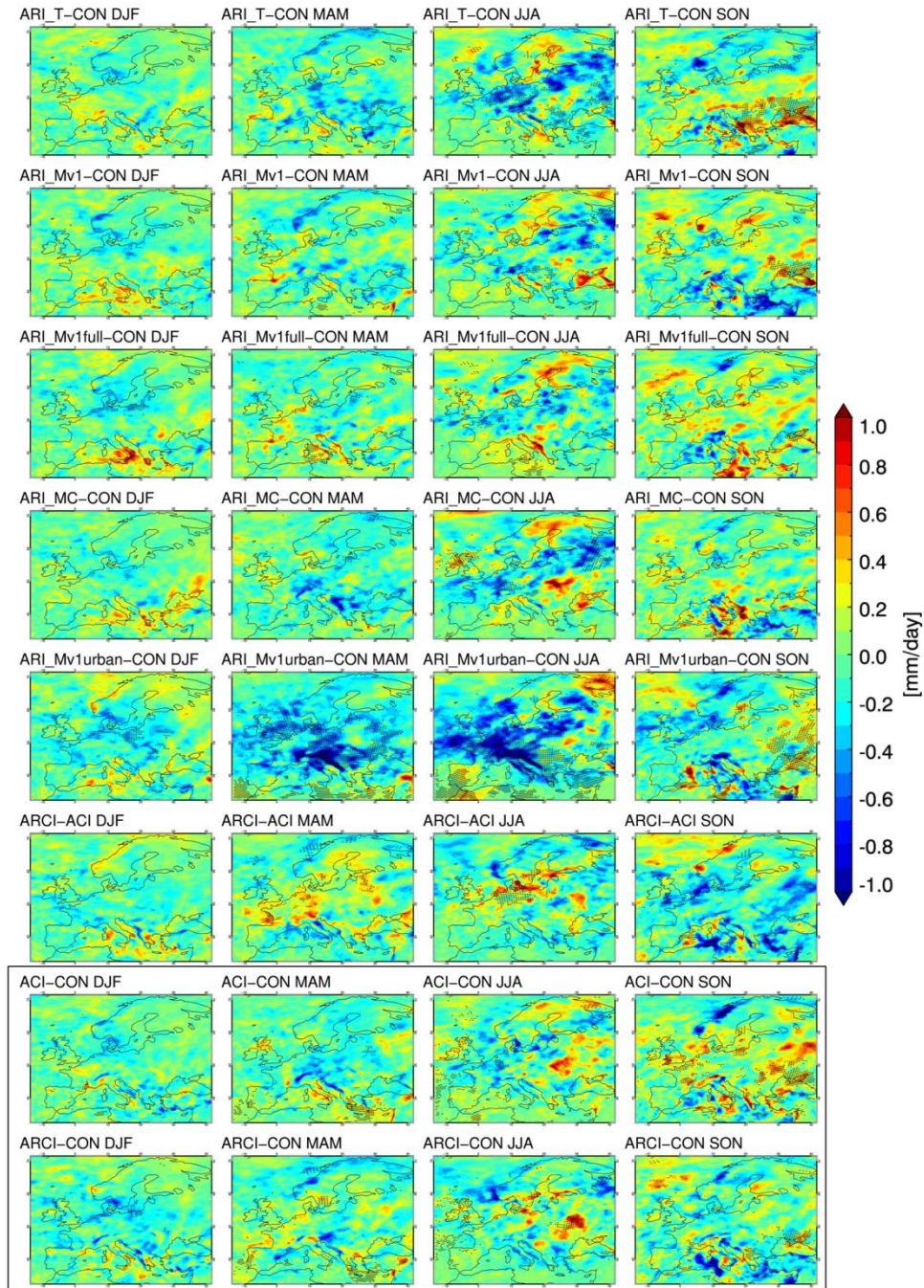


Figure S4: Precipitation difference (mm/day) difference from control simulation CON for all experiments and seasons. Furthermore the precipitation difference of ARCI calculated against ACI (ARCI-ACI) is given to assess aerosol-radiation interactions implementation in the Thompson aerosol aware microphysics (row six). First six rows present the impact of aerosol-radiation interaction. Last two rows (black box) present the impact of TE2014 with indirect effect against control (row seven) and TE2014 with aerosol-radiation interactions enabled against control (row eight). Stippling indicates areas where the differences are statistically significant at the 95% level, according to the Mann-Whitney non parametric test.

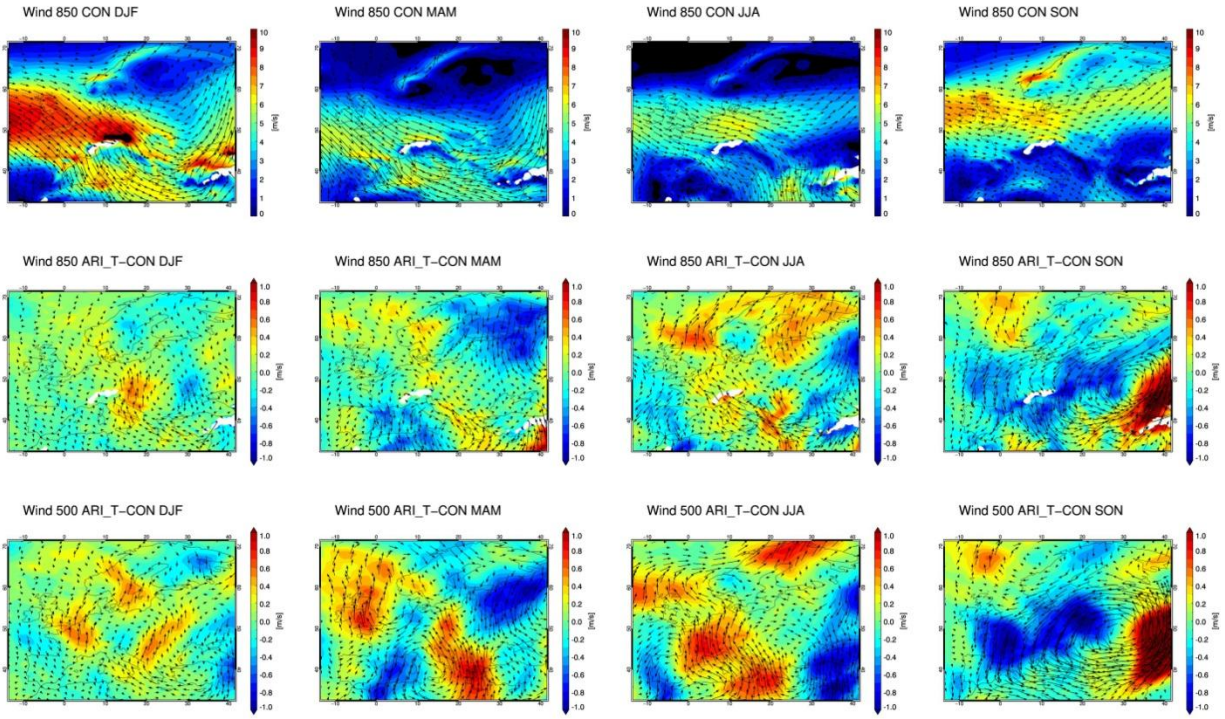


Figure S5: First row depicts the wind field (arrows) and wind speed (colored contours) of the control experiment for each season. Second row depicts the wind field anomalies (arrows) and meridional wind difference (colored contours) of simulation ARI_T from control CON at 850hPa. Likewise for the 500hPa level at the bottom row. Stippling indicates areas where the differences are statistically significant at the 95% level, according to the Mann-Whitney non parametric test.

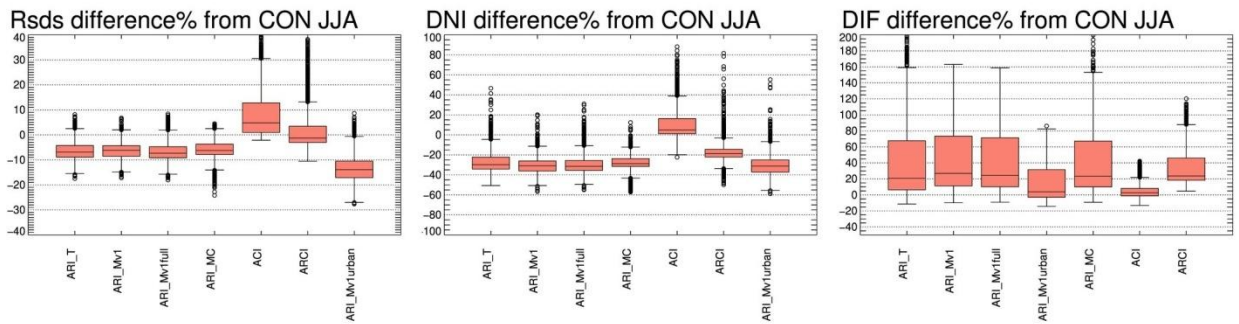


Figure S6: Plots of relative differences of the aerosol including simulations from control CON regarding the grid points of the domain during JJA. For shortwave radiation at the surface (Rsds), direct normalized irradiance (DNI) and diffuse radiation at the surface (DIF).

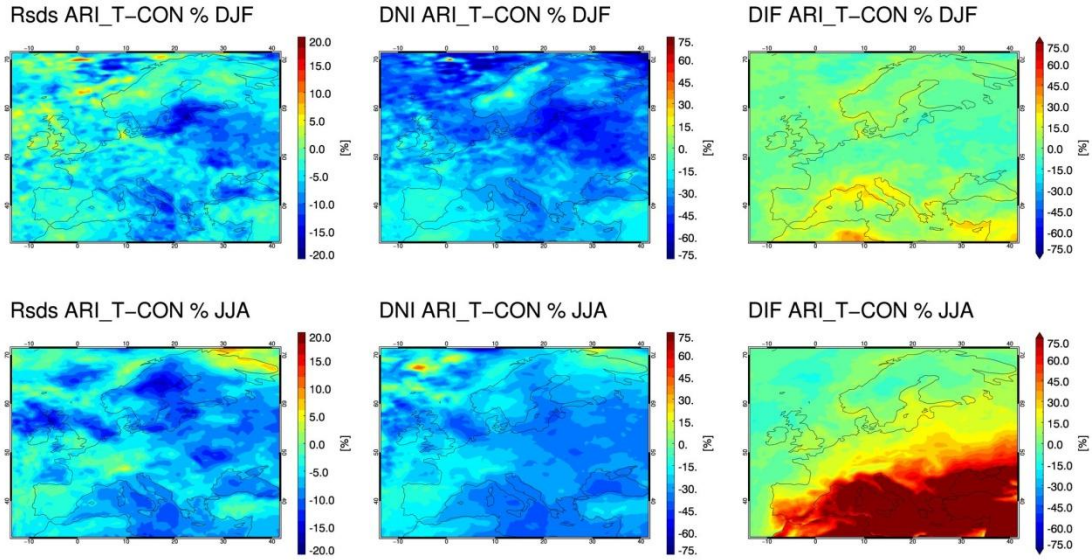


Figure S7: Relative difference, between simulations ARI_T and CON (control), for downwelling shortwave radiation to the surface (RSDS-left), Direct normal irradiance to the surface (DNI-center) and diffuse radiation to the surface (DIF-right) for winter (top) and summer (bottom).

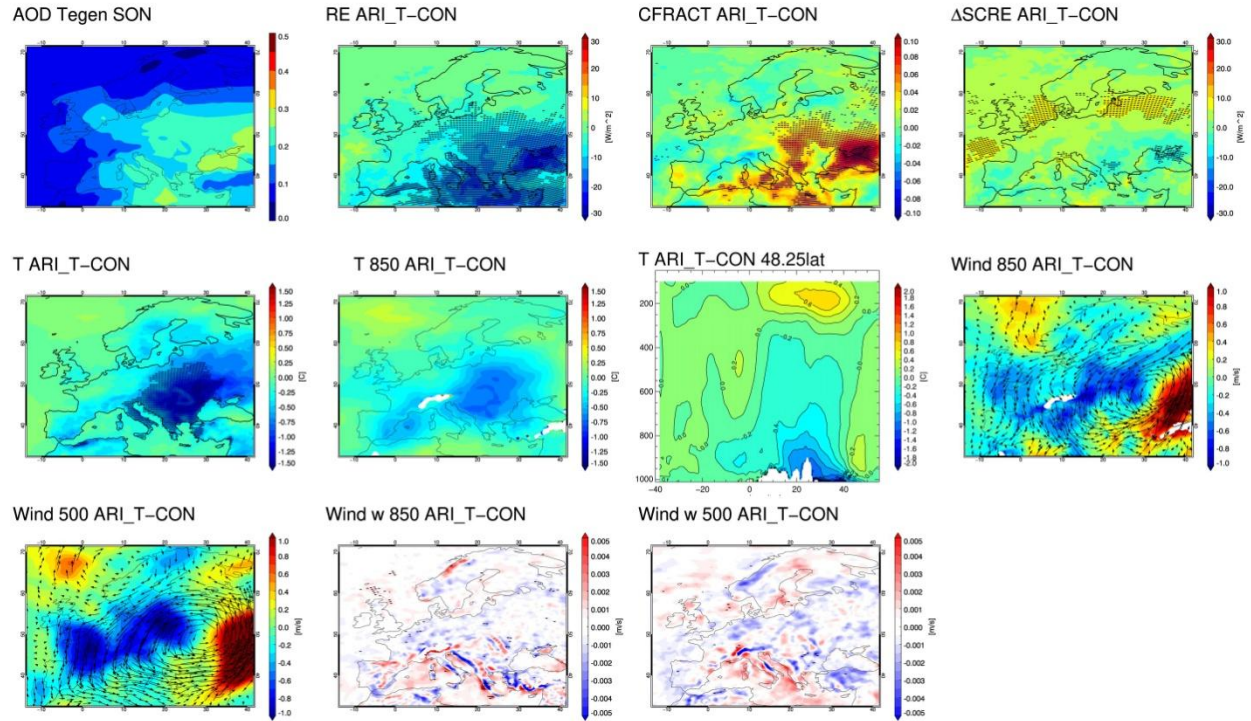


Figure S.8: Composite analysis for ARI_T in SON. All differences are calculated from CON. Top row, from left to right: AOD field, Radiative forcing RE, difference in cloud fraction CFFRACT. Second row: Differences in cloud forcing SCRE, cross-section at 48.25 latitude depicting differences in temperature vertical profile, Temperature differences at 850hPa. Third row: Difference in near-surface temperature (TAS), wind field at 850hPa, differences at the wind field at 850hPa. Bottom row: Difference in vertical wind speed w at 850hPa (left) and at 500hPa (right). Stippling indicates areas of statistical significance.

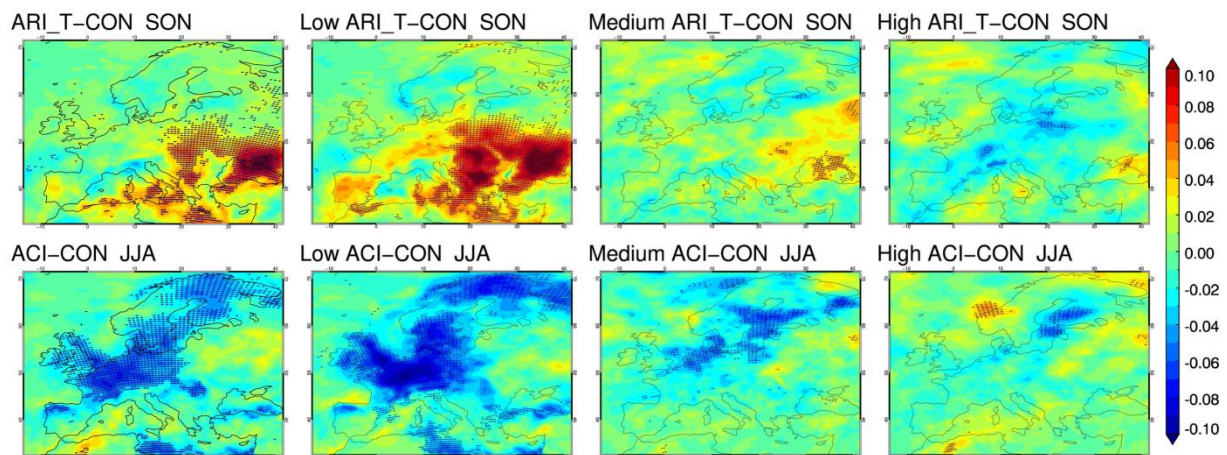


Figure S.9: Difference from control simulation CON regarding total cloud fraction (first column) as well as cloud fraction for Low, Medium and High clouds (second to fourth column respectively) for simulation ARI_T during Autumn (top row) and simulation ACI during summer (bottom row). For the period 2004-2008. Stippling indicates areas where the differences are statistically significant at the 95% level, according to the Mann-Whitney non parametric test.